PROCEEDINGS OF SCIENCE

# QCD at colliders

**Katharina Müller**[*†]
*University of Zurich*
*E-mail:* kmueller@physik.uzh.ch

Recent measurements from the ATLAS, CMS and LHCb collaborations are testing QCD with unprecedented precision and in a new energy regime. Inclusive jet, isolated photon, vector boson and heavy quark production cross section measurements are reported here including a selection of first results at the new frontier collision energy of 13 TeV.

*XXIV International Workshop on Deep-Inelastic Scattering and Related Subjects*
*11-15 April, 2016*
*DESY Hamburg, Germany*

[*]Speaker.
[†]On behalf of the ATLAS, CMS and LHCb collaborations.





PoS(DIS2016)004

## 1. Introduction

Quantum Chromo Dynamics (QCD) is a very successful theory, tested over decades in many experiments. Currently, (next-to-)next-to-leading (N)NLO calculations exist for most processes, electroweak corrections have been computed and high precision experimental results are available. Higher-order processes can still play a role in some regions of phase space, in particular for multi parton final states, and scale uncertainties still play an important role. Non-perturbative effects are important, like Parton Distribution Functions (PDF), parton showers and hadronisation.

The LHC has been providing collisions of protons at different centre of mass energies, reaching with Run 2 the unprecedented centre of mass energy of $\sqrt{s}$ of 13 TeV in $pp$ collisions. A detailed understanding of QCD is important for almost all physics processes studied by the experiments ATLAS, CMS and LHCb at the LHC[1] and essential for characterising background processes for measurements of and searches for rare or new processes. This paper summarises recent results on production of jets, isolated photons, vector bosons and heavy quarks from the LHC experiments. Measurements of multi parton final states and complex variables, as well as combinations of measurements taken at different energies probe predictions with high precision and provide input for the determination of the PDFs of the proton.

## 2. Jet production

The production of particle jets provides a testing ground for QCD, where jet production is interpreted as the showering of quarks and gluons produced in the scattering process followed by their subsequent hadronisation. At high transverse momenta[2], $p_T$, the scattering of partons can be calculated using perturbative QCD (pQCD). Jet observables, with small theoretical scale uncertainties and reduced jet energy scale uncertainty, can be used to measure the strong coupling constant $\alpha_s$. Analyses using jets at LHC generally use the anti-k$_T$ jet algorithm [1] with different jet size parameters ranging between 0.4 and 0.7. Jets of different sizes are affected differently by the impact of the non-perturbative effects of hadronization and the underlying event.

A measurement by CMS of the double differential cross section as a function of $p_T$ in different rapidity ($y$) bins of the jets at $\sqrt{s} = 8$ TeV is shown in Fig. 1 (left) [2]. The data are consistent with predictions at NLO for a wide range of jet $p_T$ from 74 GeV up to 2.5 TeV. However different PDF sets differ from each other and from the data significantly in the high $p_T$ region. Therefore this data will provide valuable input for the PDFs at high and moderate values of momentum fractions $x$ of the partons. First measurements of jet production at $\sqrt{s} = 13$ TeV are available by ATLAS [3] and CMS [4] with similar observations.

Studies of multi-jet production are crucial to understand backgrounds for searches. Theoretical calculations are challenging as the corresponding Feynman diagrams require several vertices even at tree level. Figure 1 (right) shows an ATLAS measurement of the four-jet differential cross section as a function of the invariant mass of the four jets [5]. The NLO predictions BlackHat/Sherpa [6] and NJet/Sherpa [7] tend to overestimate the cross section at large invariant masses while the all-orders calculation HEJ [8] describes the shape well but is slightly too large in normalisation.

[1] Results from CDF and DO at Tevatron have been discussed in the talk but are not presented in this paper.

[2] Natural units with = c = 1 are used throughout.

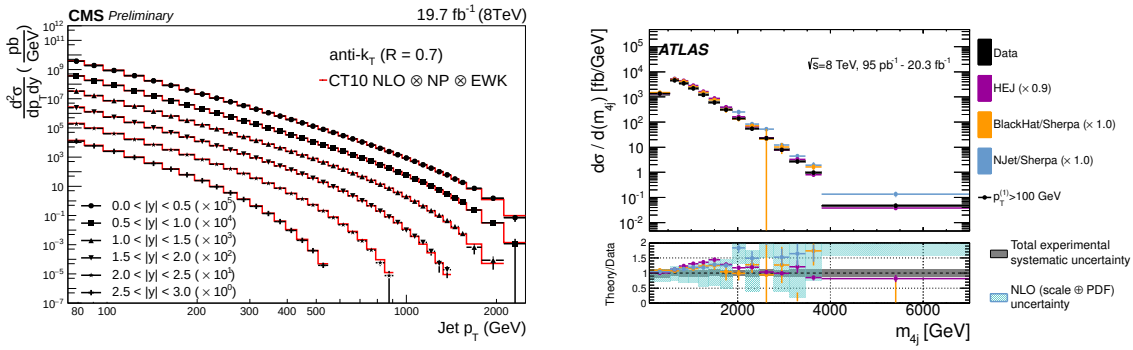


**Figure 1:** Left: Double differential jet cross section as a function of $p_T$ in different rapidity bins as measured by CMS at $\sqrt{s} = 8$ TeV [2]. Right: Measurement of the four-jet differential cross section by ATLAS as a function of the invariant mass of the four jets [5].

## 3. Isolated photons

Measurements using isolated photons and jets are complementary to each other as measurements with photons test pQCD in a cleaner experimental environment and are affected differently by hadronisation and fragmentation effects. However, backgrounds are higher, mainly from jet events with highly energetic $\pi^0$ which mimic a single photon. At LHC isolated photons are produced through the dominant leading-order process $qg \to q\gamma$. The measurements can therefore be used to study the gluon PDF of the proton. In addition, an improved understanding of the production is important as isolated photons are a significant source of background for many searches. Photon production is sensitive to the emission of soft gluons in the initial state and to the non-perturbative fragmentation of quarks and gluons to photons in the final state. Due to this rich phenomenology, theoretical predictions are challenging especially in restricted regions of phase space.

Figure 2 shows the differential cross section for isolated photon production at $\sqrt{s} = 8$ TeV [9] measured by ATLAS as a function of the transverse energy, $E_T^\gamma$, for four regions of pseudorapidity, $\eta$. It is compared to the NLO prediction from JetPhox [10] and the LO plus parton shower predictions from PYTHIA [11] and SHERPA [12]. The JetPhox predictions have a similar shape but lie below the data, while the LO predictions show different trends with the largest differences at low $E_T^\gamma$ where contributions from fragmentation dominate. The experimental precision is very high and better than the theoretical one except for high $E_T^\gamma$. First studies of isolated photon production at a $\sqrt{s} = 13$ are available and show that the shape of the observed kinematic distributions is well reproduced by the predictions [13].

Di-photon production is the main source of background to the measurement of the Higgs boson decaying into two photons. At LO di-photons are produced at LHC via $q\bar{q} \to \gamma\gamma$; at higher orders $gg \to \gamma\gamma$ contributes significantly to the cross section. Figure 3 (left) shows the di-photon cross section measured by CMS as a function of the $p_T$ of the di-photon system at $\sqrt{s} = 7$ TeV [14]. Predictions which include NNLO corrections (for example 2$\gamma$NNLO [15]) describe the shape and the normalisation of the measurement, except at very low $p_T^{\gamma\gamma}$, whereas NLO predictions ( DIPHOX + GAMMA2MC [16]) do not describe the shoulder at around 50 GeV and significantly underestimate the high $p_T^{\gamma\gamma}$ tail, the region which is most sensitive to higher-order corrections.

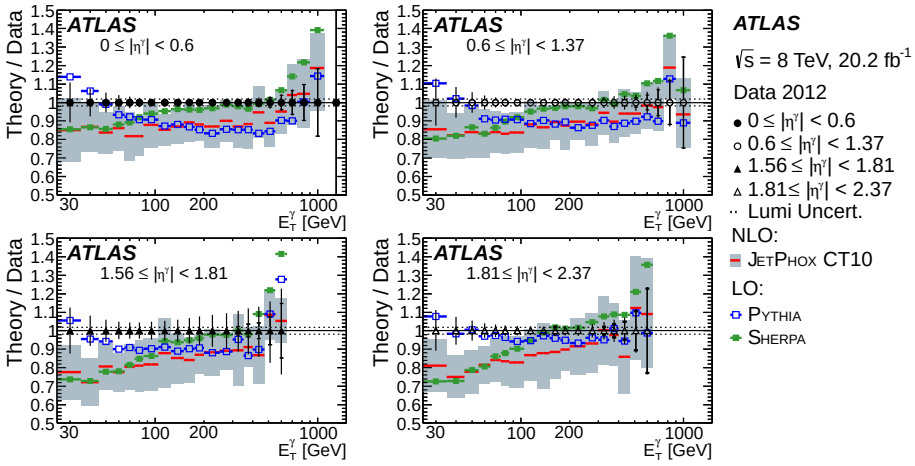


**Figure 2:** Ratio of theory to data for the differential cross sections of isolated photons as a function of $E_T^\gamma$ for four $|\eta|$ regions as measured by ATLAS [9]. The total error bar corresponds to the combined statistical and systematic uncertainty (excluding the uncertainty from the luminosity which is displayed as a dotted line). The NLO total uncertainty from JetPhox is displayed as a band.

Di-photon plus jet production is the major background source for the analysis of the Higgs boson in the di-photon decay channel, when produced via vector boson fusion. Moreover, new physics processes may lead to deviations from the predicted di-photon spectrum in events with jets in the final state. For these reasons validating the event generators for di-photon plus jet production is very important. While the predictions agree with data for a large set of differential observables, including jet multiplicity and jet spectra, differences are observed for the angular correlations between photons and jets at $\sqrt{s} = 7\,\text{TeV}$ as shown in Fig. 3 (right) [17]. Here the separation in $R = \sqrt{(\Delta\phi)^2 + (\Delta\eta)^2}$ between the leading jet and the leading photon, with $\Delta\phi$ the azimuthal separation, is shown together with the predictions from the LO and NLO event generators SHERPA [12] and aMC@NLO [18] which describe the shape within uncertainties while the fixed-order (NLO) parton-level GOSAM [19] prediction, corrected for hadronisation effects, fails to predict the measured shape.

## 4. Vector bosons

Events with $W$ and $Z$ bosons decaying into two leptons provide clean experimental signatures and allow for an efficient selection. Since the cross sections are known at NNLO with uncertainties at the percent level, measurements with vector bosons provide fundamental input for the determination of PDFs. The NNLO predictions agree with the measurements over the full kinematic range probed so far [20, 21, 22, 23, 24, 25]. Figure 4 (left) shows as an illustration the dependence of the $W$ cross section measured by ATLAS as a function of $\sqrt{s}$ together with NNLO predictions [23].

The $\phi^\star = \tan((\pi - \Delta\phi)/2) \cdot \cosh(\Delta\eta/2)$ distribution is used as a probe for the $p_T$ of the $Z$ boson. Since $\phi^\star$ has only angular variables in its definition, a very accurate experimental result can be achieved, allowing for precise comparisons with resummation techniques or with different expansions in the perturbation theory. Figure 4 (right) shows the ratio between prediction and the

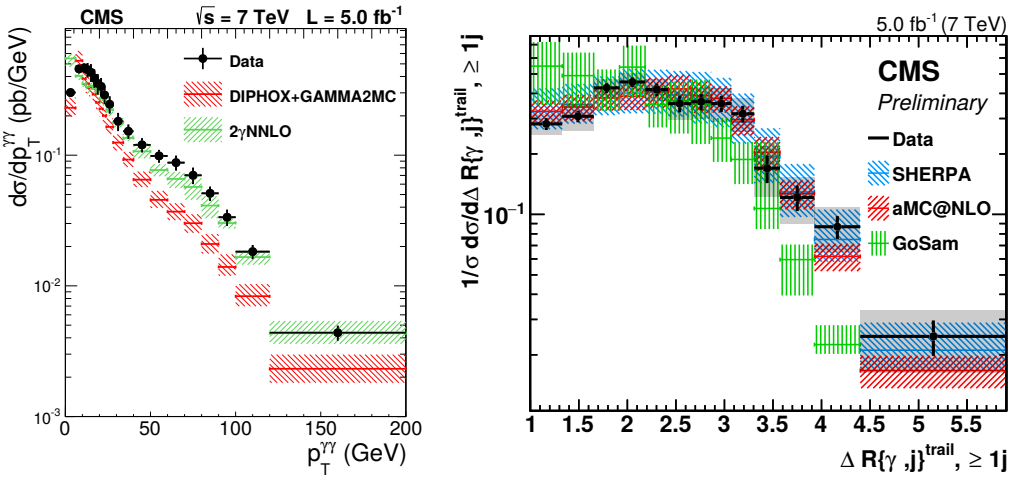


**Figure 3:** Left: Differential di-photon cross section measured by CMS as a function of $p_T^{\gamma\gamma}$ [14]. Right: Normalised differential di-photon plus jet cross section measured by CMS as a function of $\Delta R$ between the leading jet and the leading photon [17].

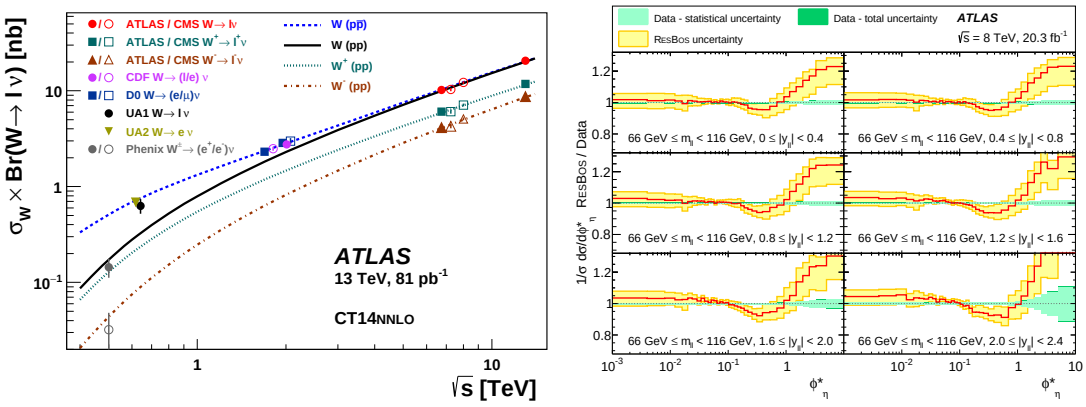


**Figure 4:** Left: Measurements by ATLAS of the total $W$, $W^+$ and $W^-$ cross sections times branching fractions versus $\sqrt{s}$ [23]. Right: Ratio between ResBos and the measurement of the normalised cross section by ATLAS as a function of $\phi^\star$ in different rapidity bins of the $Z$ [26].

measurement by ATLAS of the normalised cross section as a function of $\phi^\star$ at $\sqrt{s} = 8\,\text{TeV}$ in different rapidity bins of the di-lepton for the mass in the range of the $Z$ boson mass [26]. For values of $\phi^\star < 2$ the predictions from ResBos [27] (NLO prediction with resummation at next-to-next-to-leading-log accuracy) are consistent with the data. The experimental uncertainties are much lower than the theoretical uncertainties. However, at larger values of $\phi^\star$ the ResBos predictions are significantly higher than the data which might be due to a lack of NNLO QCD corrections for the contributions from $\gamma^\star$ and from $Z/\gamma^\star$ interference.

The $W$ charge asymmetry, $A = (\sigma(W^+) - \sigma(W^-))/(\sigma(W^+) + \sigma(W^-))$, is sensitive to the valence and sea quark contributions in the proton PDF, particularly in the forward rapidity region. CMS and LHCb measurements of $A$ in bins of the lepton pseudorapidity are presented in Fig. 5 in comparison with NNLO predictions using different PDF sets [21, 22].

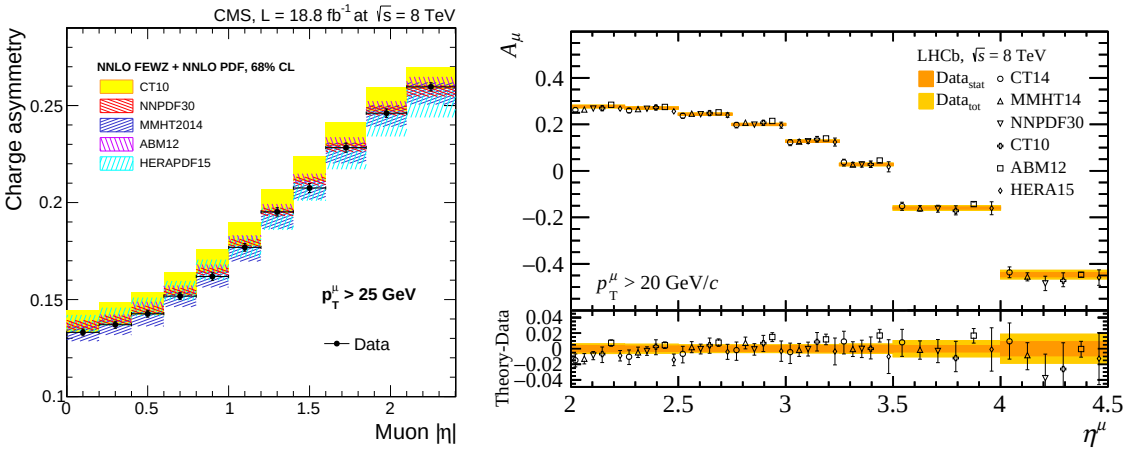


**Figure 5:** $W$ charge asymmetry as a function of the muon pseudorapidity in comparison with NNLO predictions using different PDF sets measured by CMS in the central [21] (left) and LHCb in the forward [22] (right) region.

The angular distributions of charged lepton pairs from $Z/\gamma^\star$ decays allow a precise measurements of the production dynamics through spin correlation effects between the initial-state partons and the final-state leptons predominantly mediated by the $Z$ boson when measured with an invariant mass about the $Z$-pole. Precise measurements of the angular distributions are obtained as a function of $p_T$ as well as of $y$ of the $Z$ boson [28]. The production cross section is decomposed into nine harmonic polynomials and dimensionless angular coefficients ($A_0$-$A_7$), where in each term the angular coefficients describing the production dynamics are factorised from the decay dynamics. Figure 6 (left) shows an ATLAS measurement of the difference $A_0 - A_2$, which is sensitive to the polarisation of the $Z$ boson, as a function of $p_T^Z$. The data confirm that the Lam-Tung relation ($A_0 - A_2 = 0$) does not hold, as expected. For $p_T^Z > 50$ GeV, significant deviations from zero, almost a factor of two larger than the predictions at $\mathcal{O}(\alpha_s^2)$ from DYNNLO [29] and POWHEG [30] ($\mathcal{O}(\alpha_s)$ plus parton showers) is observed, indicating that higher-order QCD corrections are required to describe the data.

Neutral current high mass Drell-Yan (DY) production is dominated by the electromagnetic quark couplings to the virtual photon $\gamma^\star$, therefore the measurements have different sensitivity to the up-type and down-type quark components of the proton PDF than measurements of $Z$ boson production. At large invariant mass the measurements constrain the antiquark PDFs at large momentum fractions $x$ which are poorly known. In addition, off-shell measurements are also sensitive to the largely unconstrained photon PDF through the photon-induced (PI) process $\gamma\gamma \to \ell^+\ell^-$. Figure 6 (right) shows the ATLAS measurement of the single-differential cross section at $\sqrt{s} = 8$ TeV as a function of the invariant mass of the lepton pair for di-lepton masses in the range $116 < m_{\ell\ell} < 1500$ GeV [31]. The cross section falls rapidly over five orders of magnitude as $m_{\ell\ell}$ increases by about a factor of ten. The data is well described by NNLO predictions which include NLO electroweak corrections. In particular at low $m_{\ell\ell}$, the differences between predictions using different PDF sets are larger than the total uncertainty of the measurement, indicating the sensitivity of the data to the PDFs and the potential to constrain them. PI processes contribute up to

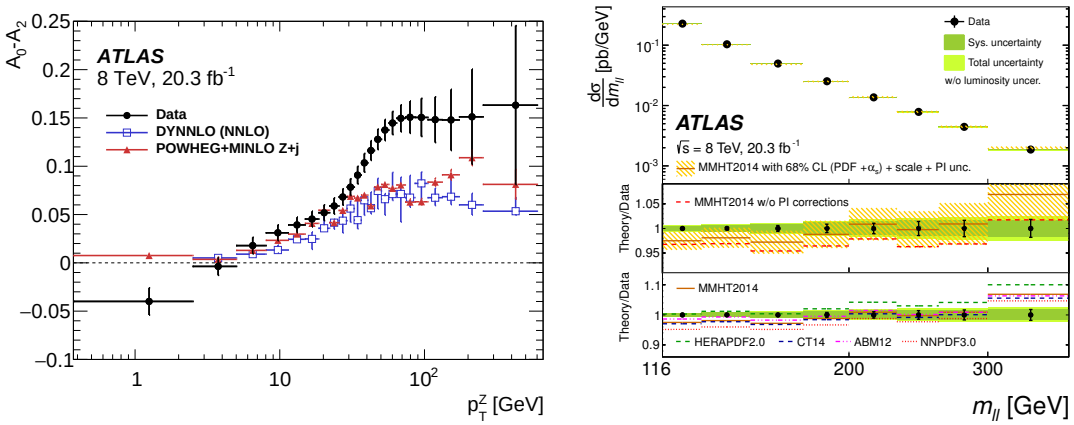


**Figure 6:** Left: ATLAS measurement of the angular coefficients $A_0 - A_2$ as a function of $p_t^Z$, compared to the DYNNLO and POWHEG predictions [28]. Right: Single-differential Drell-Yan cross section measured by ATLAS as a function $m_{\ell\ell}$ compared to NNLO predictions.The two ratio panels show the ratio of the calculation, both with and without the photon induced contribution with respect to data (middle panel), as well as the ratio for calculations using different PDFs (bottom panel) [31].

15% to the total cross sections with large uncertainties. The impact of this data on existing photon PDF sets was investigated using Bayesian reweighting [32]. Figure 7 (left) shows the photon PDF with and without including the high mass DY data from LHC. The reduction of uncertainties is large and confirms the strong sensitivity of this data to the photon PDF.

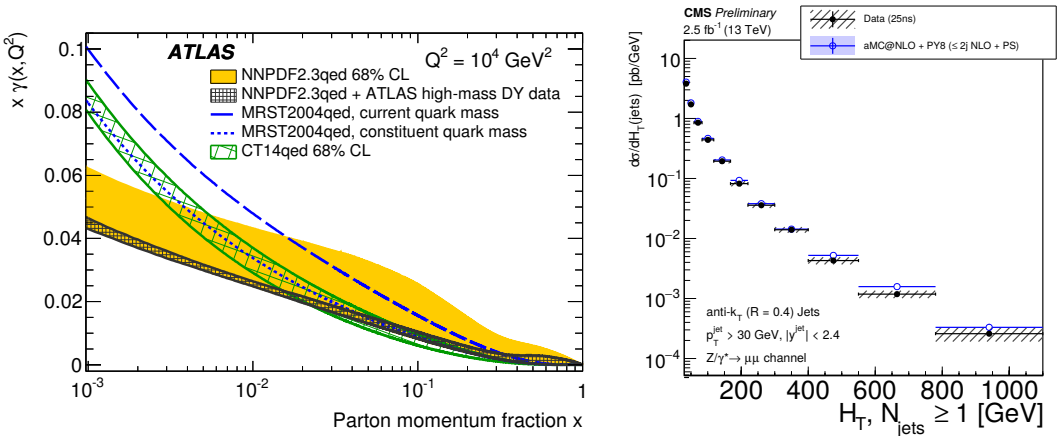


**Figure 7:** Left: The 68% confidence level interval of the NNLO photon PDF as a function of momentum fraction $x$ at the input scale $Q^2 = 104\,\mathrm{GeV}^2$ before (yellow solid area) and after (grey shaded area) inclusion of the high mass Drell-Yan measurement from ATLAS [31]. Right: CMS cross section measurement for $Z$ plus jet production as a function of $H_T$, the scalar sum of the transverse momenta of the jets [34].

## 5. Vector bosons plus jets

The production of a vector boson associated with hadronic jets is a crucial process at the LHC, which provides a reference both for pQCD measurements and detector response. Furthermore, the

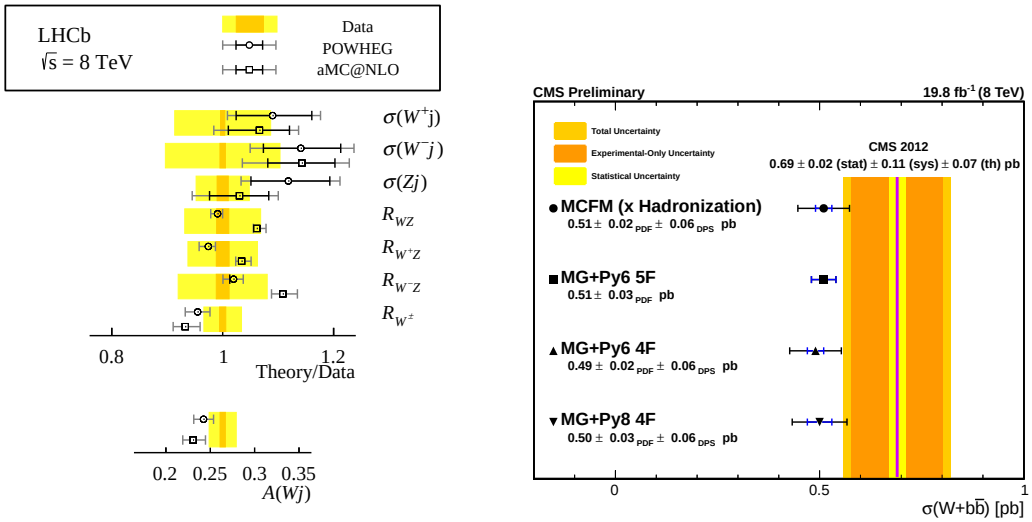


**Figure 8:** Left: Summary of vector boson plus jet production in the forward region at $\sqrt{s} = 8$ TeV by LHCb. The cross sections and ratios are shown normalised to the measurement, while the asymmetry is presented separately [35]. Right: CMS measurement of the $W + b\bar{b}$ cross section at $\sqrt{s} = 8$ TeV [36].

$W/Z$ plus jets process is a dominant background for processes such as top quark production and Higgs physics precision measurements as well as for searches for new physics. The purity and sensitivity for these relatively rare processes can be improved if vector boson plus jets processes are known precisely enough, which can also help to constrain the theoretical modelling of data.

First measurements of $Z$ plus jet production at $\sqrt{s} = 13$ TeV are available [33, 34]. The measured cross sections are compared to NLO predictions from aMC@NLO [18] with parton shower which show a reasonable agreement with the observed cross section. As an example Fig. 7 (right) shows the $H_T$ distribution measured by CMS, where $H_T$ is the scalar sum of the $p_T$ of the jets. In the forward region $W$ and $Z$ production with jets is measured at $\sqrt{s} = 8$ TeV [35]. The bosons are reconstructed in the muonic decay channel with the muon in the range $2 < \eta < 4.5$. The measured cross sections, ratios and the $W$ charge asymmetry are shown in Fig. 8 (left) and found to be in good agreement with fixed order $\mathcal{O}(\alpha_s^2)$ predictions from POWHEG [30] and aMC@NLO [18]. Figure. 8 (right) shows the cross section for $W$ plus two $b$-tagged jets measured by CMS at $\sqrt{s} =$ 8 TeV [36]. Standard model predictions from MadGraph [37] and MCFM [38], corrected for hadronisation effects, agree with the data at the level of one standard deviation.

## 6. Heavy quark production

Many new measurements of heavy quark production are available by the LHC experiments; these test pQCD predictions at lower scales than the measurements presented in the previous sections and provide input for PDF fits in a different kinematic region. Measurements of charm and $J/\Psi$ production at $\sqrt{s} = 13$ TeV have been performed by LHCb in the forward region [39, 40]. The shapes of the differential cross sections for $D^0$, $D^{(\star)+}$, and $D^{s+}$ mesons are found to be in agreement with fixed order, next-to-leading-log (FONLL [41]) predictions while the predicted central values as well as the ratios of the production cross sections, $R_{13/7}$, for $\sqrt{s} = 13$ and 7 TeV generally

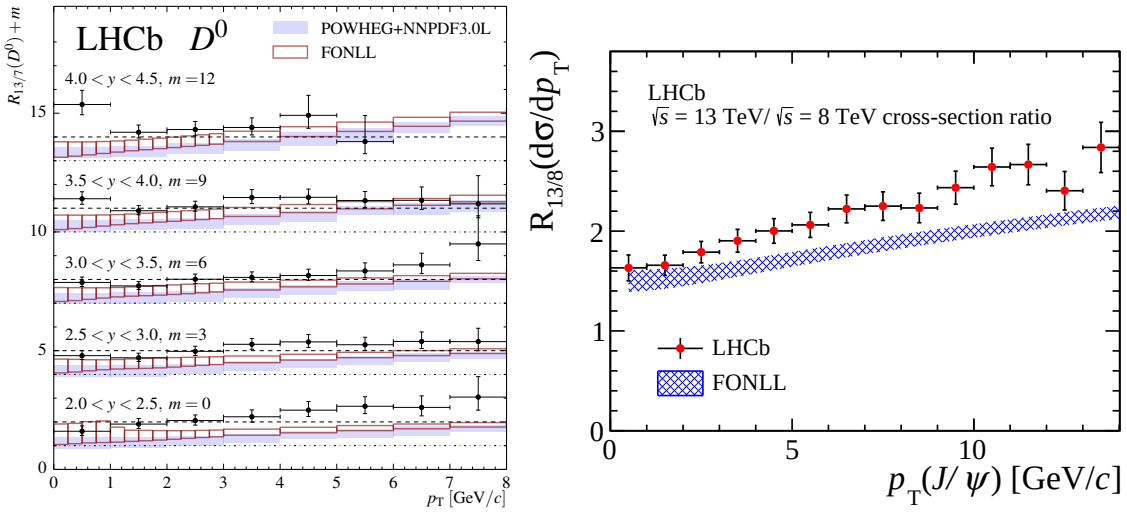


**Figure 9:** Left: Ratio $R_{13/7}$ for prompt $D^0$ as a function of $p_T$ for different rapidity bins of $D^0$ [39]. Right: Ratio $R_{13/8}$ for $J/\Psi$ from $b$-hadron decays as a function of $p_T$ [40].

lie below the data (Fig. 9 (left)) [39]. Since the results at 7 TeV agree well with predictions this indicates that the level of agreement worsens with the increase in collision energy. $J/\Psi$ production was studied for prompt $J/\Psi$ and for $J/\Psi$ from $b$-hadron decays. The $p_T$ distribution of $J/\Psi$ mesons produced at $\sqrt{s} = 13$ TeV is harder than that at $\sqrt{s} = 8$ TeV and in agreement with FONLL predictions, while the ratio $R_{13/8}$ of the cross sections at $\sqrt{s} = 13$ and 8 TeV is underestimated (see Fig. 9 (right)).

## 7. Summary

Many new high precision QCD measurements with different final states are available from the LHC experiments ATLAS, CMS and LHCb . These explore regions of phase space where current predictions still struggle to match the data. The combination of measurements taken at different centre of mass energies further allows for more stringent test of the predictions since many uncertainties cancel. A systematic exploration of all the final states and centre of mass energies will largely improve our understanding of QCD.

## References

[1] M. Cacciari, G. P. Salam and G. Soyez, JHEP **0804** (2008) 063.

[2] CMS collaboration, CMS-PAS-SMP-14-001.

[3] ATLAS collaboration, ATLAS-CONF-2015-034.

[4] CMS collaboration, CMS-PAS-SMP-15-007.

[5] G. Aad *et al.* [ATLAS Collaboration], JHEP **1512** (2015) 105

[6] C. Berger *et al.*, Phys. Rev. **D78** (2008) 036003, Z. Bern *et al.*, Phys. Rev. Lett. **109** (2012) 042001.

[7] S. Badger *et al.*, Comput. Phys. Commun. **184** (2013) 1981.

[8] J. R. Andersen and J. M. Smillie, JHEP **06** (2011) 010.

[9] G. Aad *et al.* [ATLAS Collaboration], arXiv:1605.03495 [hep-ex].

[10] S. Catani*et al.*, JHEP 0205 (2002) 028.

[11] T. Sjöstrand, S. Mrenna and P. Z. Skands, Comp. Phys. Comm. 178 (2008) 852.

[12] T. Gleisberg *et al.*, JHEP 0902 (2009) 007.

[13] ATLAS Collaboration, ATL-PHYS-PUB-2015-016

[14] S. Chatrchyan *et al.* [CMS Collaboration], Eur. Phys. J. C **74** (2014) no.11, 3129.

[15] S. Catani *et al.*, Phys. Rev. Lett. **108** (2012) 072001.

[16] T. Binoth, J. P. Guillet, E. Pilon, and M. Werlen, Eur. Phys. J. C **16** (2000) 311, Z. Bern, L. J. Dixon, and C. Schmidt, Phys. Rev. D **66** (2002) 074018.

[17] CMS collaboration, CMS-PAS-SMP-14-021.

[18] J. Alwall *et al.*, JHEP **1407** (2014) 079

[19] T. Gehrmann, N. Greiner, and G. Heinrich, JHEP **1306** (2013) 058

[20] G. Aad *et al.* [ATLAS Collaboration], Phys. Rev. D **85** (2012) 072004.

[21] V. Khachatryan *et al.* [CMS Collaboration], arXiv:1603.01803 [hep-ex].

[22] R. Aaij *et al.* [LHCb Collaboration], JHEP **01** (2016) 155

[23] G. Aad *et al.* [ATLAS Collaboration], Phys. Lett. B **759** (2016) 601.

[24] CMS collaboration, CMS-PAS-SMP-16-004, CMS collaboration, CMS-PAS-SMP-15-011

[25] LHCb collaboration, arXiv:1607.06495 [hep-ex].

[26] G. Aad *et al.* [ATLAS Collaboration], Eur. Phys. J. C **76** (2016) no.5.

[27] C. Balazs, J.-W. Qiu, C. Yuan, Phys. Lett. B **355**, 548-554 (1995).

[28] G. Aad *et al.* [ATLAS Collaboration], arXiv:1606.00689 [hep-ex].

[29] S. Catani *et al.* Phys. Rev. Lett. **103** (2009) 082001

[30] S. Alioli *et al.*, JHEP **06** (2010) 043.

[31] G. Aad *et al.* [ATLAS Collaboration], arXiv:1606.01736 [hep-ex].

[32] W. T. Giele and S. Keller, Phys. Rev. D 58 (1998) 094023.

[33] ATLAS Collaboration, ATLAS-CONF-2015-041

[34] CMS collaboration, CMS-PAS-SMP-15-010

[35] R. Aaij *et al.* [LHCb Collaboration], JHEP 05 (2016) 131.

[36] CMS collaboration, CMS-PAS-SMP-14-020.

[37] F. Maltoni and T. Stelzer, JHEP 02 (2003) 027.

[38] J. M. Campbell and R. Ellis, Nucl.Phys.Proc.Suppl. 205 (2010) 10.

[39] R. Aaij *et al.* [LHCb Collaboration], JHEP **1603** (2016) 159.

[40] R. Aaij *et al.* [LHCb Collaboration], JHEP 10 (2015) 172.

[41] M. Cacciari, M. Greco, and P. Nason, JHEP **05** (1998) 007.